J. Chem. Sci. Vol. 128, No. 11, November 2016, pp. 1813–1821. © Indian Academy of Sciences.
DOI 10.1007/s12039-016-1163-4

Synthesis, Spectroscopic Properties and DFT Calculation of Novel Pyrrolo[1′,5′-a]-1,8-naphthyridine Derivatives through a Facile One-pot Process

GAO-ZHANG GOU[a], BO ZHOU[a], HE-PING YAN[a], YONG HONG[a], WEI LIU[a], SHAO-MING CHI[b] and CHAO-YONG MANG[c,*]

[a]School of Science, Honghe University, Mengzi, Yunnan 661199, P. R. China
[b]College of Chemistry and Chemical Engineering, Yunnan Normal University, Kunming 650092, P. R. China
[c]College of Pharmaceutical Science and Chemistry, Dali University, Dali, Yunnan 671000, P. R. China
e-mail: hhxylxyhxx@126.com; cymang619@yeah.net

MS received 15 June 2016; revised 30 July 2016; accepted 8 August 2016

Abstract. Novel pyrrolo[1′,5′-a]-1,8-naphthyridine compounds (**L1**-**L4**) have been synthesized through a facile one-pot process by the reaction of the corresponding 1,8-naphthyridines with aliphatic anhydride. The structures were established by spectroscopic data. Further, X-ray crystal analysis of 7-diacetamino-2,4-dimethy-1,8-naphthyridine (**L1**) identifies its molecular structure and reveals π-π stacking. The synthetic mechanisms for **L2**, **L3** were studied by density functional theory calculations. And a comprehensive study of spectroscopic properties involving experimental data and theoretical studies is presented. **L1** exhibited electronic absorption spectrum with λ_{max} at ~320 nm. **L2**-**L4** exhibited similar electronic absorption spectra with λ_{max} at ~390 nm that is tentatively assigned to $\pi \rightarrow \pi^*$ transition. The assignment was further supported by density functional theory (DFT) calculations.

Keywords. Indolizine; 1,8-naphthyridine; density functional theory; crystal structure; spectroscopic properties.

1. Introduction

The development of new and highly efficient strategies for the rapid synthesis of intricate molecular architectures is of great importance and remains a preeminent goal in current synthetic chemistry.[1] The chemistry of fused nitrogen heterocycles is of great importance due to their wide applications.[2] As well-known fused-ring N-heterocycles, indolizines are ubiquitous scaffolds found in natural products and synthetic drugs. Several indolizines as core structures are found in many pharmacological compounds because of their interesting biological activities and physical properties.[3] Naphthyridines (pyridopyridines, diazanaphthalenes) represent a group of six isomeric heterocyclic systems containing two fused pyridine rings with different mutual arrangements of nitrogen atoms.[4] 1,8-Naphthyridine compounds have been extensively investigated not only due to their special conjugate π electronic structures, good coordination capabilities,[5] favourable photophysical and photochemical properties,[6,7] but also for their potential applications as functional materials in the fields of solar energy conversion, sensors,[8] supramolecular assemblies,[9,10] photocatalysis,[11,12] non-linear optical materials, biologically active materials,[13] optical molecular devices,[14–16] etc. The most general formation of the five-membered ring moiety in the indolizine framework is based on intramolecular condensation (Schotz reaction[17]) or intermolecular condensation (Tschitschibabin reaction[18]). The Scholtz or Tschitschibabin cyclocondensation reactions are considered as more practical because they accomplish the construction of indolizine in a one-pot procedure.[19] Therefore, extending the indolizine derivatives by incorporating a 1,8-naphthyridine aromatic ring may enlarge their application in therapeutics. And the research work on the spectroscopic properties is still very little.

In the present work, we report on the synthesis and characterization of novel pyrrolo[1′,5′-a]-1,8-naphthyridine derivatives through a facile one-pot process (Scheme 1). Their structures were established by spectroscopic data. Further, X-ray crystal analysis of 7-diacetamino-2,4-dimethy-1,8-naphthyridine (**L1**) identifies its intriguing molecular structure and reveals the strong π–π stacking. Then, the spectroscopic properties are comprehensively studied involving experimental data and time-dependent density functional theory (TD-DFT) calculations. And the synthetic mechanism was discussed.

*For correspondence

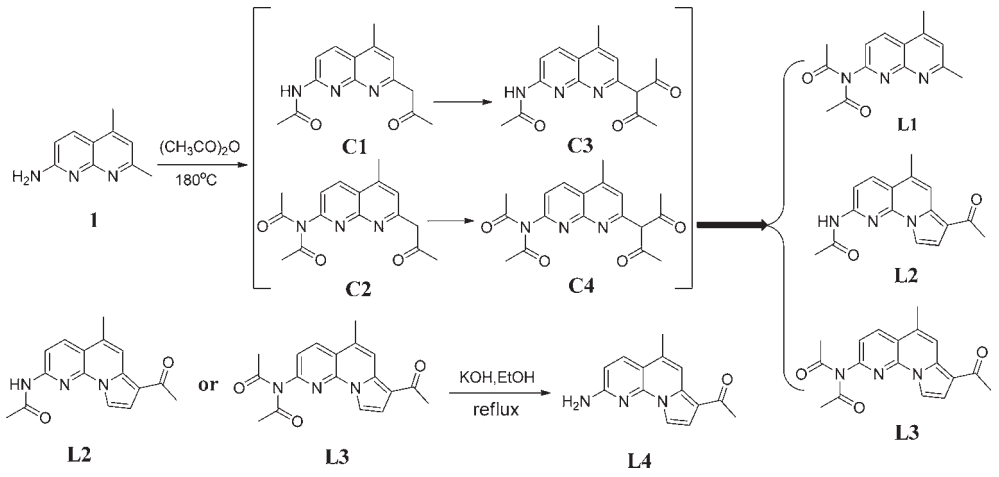

Scheme 1. Synthetic routes and chemical structures of **L1-L4**.

2. Experimental

2.1 *Instrumentation and Physical Characterization*

Flash chromatography was carried out on silica gel (200–300 mesh), ^{1}H NMR spectra were run on a Bruker Avance 500 spectrometer with tetramethylsilane (^{1}H) as the internal standard. Chemical shifts were expressed in ppm and coupling constants (J) in H_Z. Electrospray Ionization ESI mass spectra were performed on a Finnigan LCQ quadrupole ion trap mass spectrometer (samples were dissolved in HPLC grade methanol). Elemental analyses (C, H, N) were performed on a Perkin-Elmer 240 analyzer. The UV-Vis spectra were obtained using U-3010 diode array spectrophotometer. The fluorescence spectra were obtained with F-7000 FL spectrometer with a 1 cm standard quartz cell. The fluorescence quantum yields in solution were measured relative to quinine sulfate in sulfuric acid aqueous solution ($\lambda_{ex} = 345$ nm, $\Phi_F = 0.546$) at room temperature and calculated by $\Phi_s = \Phi_r(B_r/B_s)(n_s/n_r)^2(D_s/D_r)$, where the subscripts s and r refer to the sample and reference standard solution respectively, n is the refractive index of the solvents, D is the integrated intensity, and Φ is the luminescence quantum yield. The quantity B was calculated[20] by $B = 1-10^{-AL}$, where A was the absorbance/cm of the solution at the excitation wavelength and L(cm) was the optical path length (L is 1 cm in our experiments). Estimated errors for wavelength and Φ are 1 nm and 10%, respectively.

2.2 *Synthesis and Characterization*

2.2.1 *Syntheses of **L1-L3**:* A mixture of 7-amino-2,4-dimethy-1,8-naphthyridine (2.0 g, 11.5 mmol) and acetic anhydride (20 mL) was heated at 180°C for 24 h with stirring in an atmosphere of nitrogen. After the unreacted acid anhydride was evaporated under vacuum, the residue was chromatographed on a silica-gel column to give the product **L1**-**L3**.

2.2.1a **L1**: (Yield: 889 mg, 29.9%); ^{1}H NMR (500 MHz, CD_3CN) δ(ppm): 8.61 (d, $J = 8.5$ Hz, 1H Naph-H), 7.51 (d, $J = 8.5$ Hz, 1H Naph-H), 7.41 (s, 1H Naph-H), 2.73 (s, 3H -CH_3), 2.27 (s, 6H -CH_3), 2.22 (s, 3H -CH_3). ESI-MS(m/z): 258.31$[M+1]^+$. Elemental analysis calcd (%) for $C_{14}H_{15}N_3O_2$: C, 65.35; H, 5.88; N, 16.33; O, 12.44; found (%): C, 65.33; H, 5.90; N, 16.31.

2.2.1b **L2**: (Yield: 758 mg, 23.3%) ^{1}H NMR(500 MHz, $CDCl_3$) δ(ppm): 8.36 (d, $J = 8.2$ Hz, 1H Naph-H), 8.18 (d, $J = 8.8$ Hz, 1H Naph-H), 8.16 (s, 1H -NH), 8.07 (s, 1H Naph-H), 8.00 (d, $J = 3.2$ Hz, 1H Pyr-H), 7.07 (d, $J = 3.3$ Hz, 1H Pyr-H), 2.58 (s, 3H -CH_3), 2.56 (s, 3H -CH_3), 2.32 (s, 3H -CH_3). ESI-MS(m/z): 282.11$[M+1]^+$. Elemental analysis calcd (%) for $C_{16}H_{15}N_3O_2$: C, 68.31; H, 5.37; N, 14.94; O, 11.37; found (%): C, 68.28; H, 5.39; N, 14.95.

2.2.1c **L3**: (Yield: 578 mg, 15.5%) ^{1}H-NMR (500 MHz, $CDCl_3$) δ(ppm): 8.33 (d, $J = 8.7$ Hz, 2H Naph-H), 8.15 (d, $J = 3.0$ Hz, 1H Naph-H), 7.40 (d, $J = 8.2$ Hz, 1H Pyr-H), 7.12 (d, $J = 3.1$ Hz, 1H Pyr-H), 2.63 (s, 3H -CH_3), 2.59 (s, 3H -CH_3), 2.39 (s, 6H -CH_3). ESI-MS(m/z): 324.37$[M+1]^+$. Elemental analysis calcd (%) for $C_{18}H_{17}N_3O_3$: C, 66.86; H, 5.30; N, 13.00; O, 14.84; found (%): C,66.83; H, 5.28; N, 13.02.

2.2.2 *Syntheses of **L4**:* Claisen base (25.0 mL) was added to a mixture solution of **L2** (0.30 g, 1.06 mmol) and methanol (25.0 mL). And the mixture was refluxed

under nitrogen with stirring for 6 h at 60°. After the reaction, the pH of the solution was adjusted to 7 by concentrated hydrochloric acid. The solution was extracted by chloroform (3 × 50 mL). The extract was dried by sodium sulfate and the solvent was removed by rotary evaporation. The crude product was purified by column chromatography on silica gel, eluted with petroleum ether: dichloromethane (1:20) to obtain the product **L4** Yield: 0.233 g 91.4% ^{1}H NMR (500 MHz, $CDCl_3$)δ(ppm): 8.03 (s, 1H Naph-H), 8.02 (d, J = 3.3 Hz, 1H Naph-H), 7.94 (d, J = 8.6 Hz, 1H Naph-H), 7.05 (d, J = 3.3 Hz, 1H Pyr-H), 6.65 (d, J = 8.6 Hz, 1H Pyr-H), 4.85 (s, 2H NH_2), 2.54 (s, 3H -CH_3), 2.54 (s, 3H -CH_3). ESI-MS(m/z): 240.24[M+ H]$^+$. Elemental analysis calcd (%) for $C_{14}H_{13}N_3O$: C, 70.28; H, 5.48; N, 17.56; O, 6.69; found (%): C,70.31; H, 5.46; N, 17.54.

2.3 *X-ray Diffraction Studies*

Single crystals of **L1** suitable for X-ray diffraction analysis were grown by slow diffusion of diethyl ether vapor into a dichloromethane solution. The diffraction data were collected on a Rigaku R-AXIS RAPID IP X-Ray diffractometer using a graphite monochromator and MoKα radiation (λ = 0.071073 nm) at 293 K. The structures were solved by direct methods and refined by full-matrix least-squares methods on all *F2* data (SHELX-97).[21] Non-hydrogen atoms were refined anisotropically. The positions of hydrogen atoms were calculated and refined isotropically. A summary of the crystallographic parameters and data is given in Tables S1, S2 and S3 (Supplementary Information)

2.4 *Theoretical Calculations*

Gaussian 09W[22] package was used in the present computational study. All geometrical structures were fully optimized without the symmetric restraint using the DFT method[23,24] combined with the Becke, three-parameter, Lee–Yang–Parr (B3LYP) exchange-correlation functional[25–28] with the 6-311++G** basis set.[29–32] The electronically excited states involving the first 30 excited states were calculated by using the TD-DFT method. In all calculations, squeezed self-consistent field (SCF) convergence standards, the self-consistent reaction field (SCRF) method and polarized continuum model (PCM)[33,34] were adopted. The UV-Vis spectra were computed from TD-DFT calculations in different media (gas, CH_2Cl_2, Ac_2O) and molecular orbitals calculated in gas phase.

3. Results and Discussion

3.1 *Synthesis and Structures*

As outlined in Scheme 1, the precursor 7-amino-2, 4-dimethy-1,8-naphthyridine (**1**) was prepared from 2,6-diaminopyridine by the reported methods.[35,36] The synthesis of 7-diacetamino-2,4-dimethy-1,8-naphthyridine (**L1**) and pyrrolo[1′,5′-a]-1,8-naphthyridine derivatives (**L2**, **L3**) were carried out in acetic anhydride under a nitrogen atmosphere at 180°C; **L2** and **L3** are similar to indolizine. Pyrrolo[1′,5′-a]-1,8-naphthyridine compound **L4** was synthesised in 30% water-methanol mixture of KOH under a nitrogen atmosphere. The structures of **L1**-**L4** were fully characterized by multinuclear NMR spectroscopy, mass spectroscopy and elemental analyses (Figures S1-S4 in Supplementary Information). Furthermore, mass spectrum and elemental analyses revealed that compounds **L2–L4** are pyrrolo[1′,5′-a]-1,8-naphthyridines. Besides spectral data, the structure of **L1** was further confirmed by X-ray crystal analysis. Crystal structure of **L1** is depicted in Figure 1 and detailed crystallographic data is gathered in Table S1. Bond lengths, angles, torsion angles, hydrogen bonds and crystal packing diagram are shown in Tables S2–S4 and Figure S5 (Supplementary Information). Compound **L1** crystallizes in the monoclinic space group *P21/c*. The two acetamido groups are located on both sides of the 1,8-naphthyridine ring of planar geometry. The molecules stack along the *c* axis to form the layer structure (Figure S5 in SI). The distance between planes is only 3.407 Å, which is just like that of the interplanar distance in graphite (3.35 Å). This reveals that the π–π stacking system in the crystal is very strong. As shown in the figure and table (hydrogen bonds, Figure S6 and Table S4 in SI), the molecules are arranged in the plane through intermolecular hydrogen bonds linked by C(12)-H(12A)...N(1) (3.254 Å) and C(12)-H(12A)...N(2) (3.684 Å). And the length is 2.547 Å for H(12A)...N(1) and 2.726 Å for H(12A)...N(2). Although the crystal structure of compound **L2-L4** was not obtained, but similar single crystal analyses have been reported.[19]

3.2 *Reaction Process and Mechanism*

The synthetic mechanism is depicted in Scheme 2. It is proposed that acetylation of the methyl, which produces 2-methyl-7-diacetylmethyl-1,8-naphthyridine (**C3**, **C4**), is the first step. Then, a tautomeric form (**C3**, **C4**) of (**C1**, **C2**) undergoes ring closure to 3′-hydroxy-4′-acetyl-7-R-2′,3′-dihydro-pyrrolo[1′,5′-a]-1,8-naphthyridine (**a**). Finally, dehydration of **a** produces **L2**, **L3**.

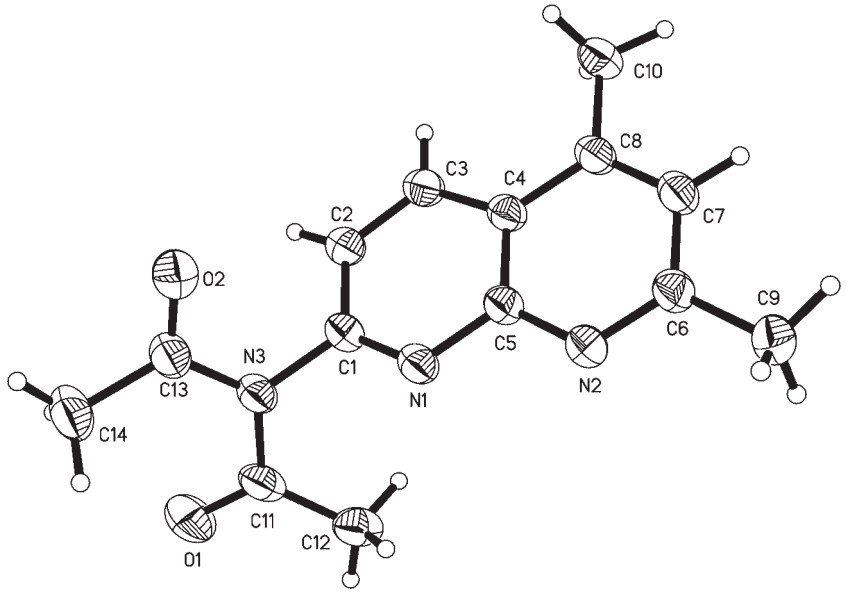

Figure 1. ORTEP diagram for **L1** showing 30% probability ellipsoids.

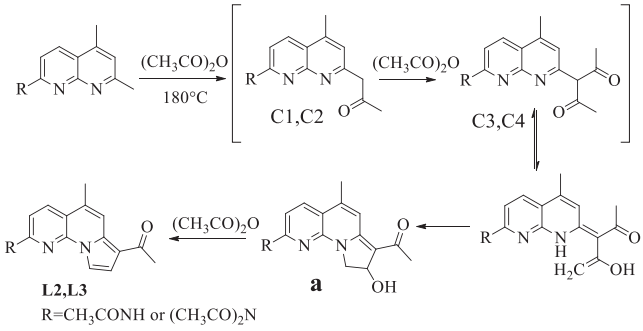

Scheme 2. The synthetic mechanism of **L2** and **L3**.

Similar synthetic mechanism has been confirmed in the literature.[19,37] From the above discussion, this reaction process may be undergoing transition state and intermediate compounds **C1**–**C4** but we failed to detect. So, the density functional theory (DFT) study was used to investigate the synthetic mechanism. The relative energies calculated at 6-311++G** level in different solvents of compounds **1**, **L1**–**L3**, **C1**–**C4** are shown in Figure 2. Based on the relative energy of **1** as indicator, the relative energies of **1**, **L1**–**L3**, **C1**–**C4** are **C3**>**L2**>**C1**>**1** and **C4**>**L3**>**C2**>**L1**>**1**. So, it can generate **L2** and **L3** theoretically from the transition state intermediate compounds **C3** and **C4**. In order to verify the reaction process and mechanism, the molecular atomic charges of 7-acetamido-2,4-dimethyl-1,8-naphthyridine (**1**) were calculated using the same method. As shown in Figure 3, the charges of 2-Me unit in compound **1** are −0.408, −0.460 and −0.471, respectively. This indicated that the 2-Me unit is more easy to react by acetylation in the solvent acetic anhydride. Although the charges for 4-Me unit is even higher (−0.537), but it is on the opposite side of the nitrogen atom and has greater distance. The effect of nitrogen atoms on 2-Me unit is greater than that of 4-Me unit.

3.3 *Electronic Absorption Spectroscopy and Photoluminescence*

The spectral properties of compounds **L1**–**L4** were examined under various conditions and the results are summarized in Table 1. As shown in Figure 4, compound **L1** in CH_2Cl_2 shows moderately intense absorption at ~320 nm. And compounds **L2**–**L4** in CH_2Cl_2 show moderately intense absorption between 350–425 nm and exhibit intense bands between 270 and 300 nm. The structured low-energy absorption bands with a large extinction coefficient (~104 $mol^{-1}\cdot dm^{-3}\cdot cm^{-1}$) may be assigned to the 0→0 vibrational band of the strong S0→S1 transition with some charge-transfer character, as evidenced by the slight sensitivity towards solvent polarity (Figure S7 in Supplementary Information). On going from **L1** to pyrrolo[1′,5′-a]-1,8-naphthyridine (**L2**–**L4**), the formation of the pyrrole ring caused a significant shift (about 72 nm) in the absorption maximum. It shows that the formation of the pyrrole ring increased the molecular conjugation.

The emission spectrum of **L1** is too weak to be accurately determined. Upon excitation at 388 nm, the emission spectra of **L2**–**L4** in CH_2Cl_2 feature a broad and structureless peak, with λ_{max} (quantum yield; Stokes shift) of 454 nm (87%; 66 nm), 454 nm (83%; 66 nm)

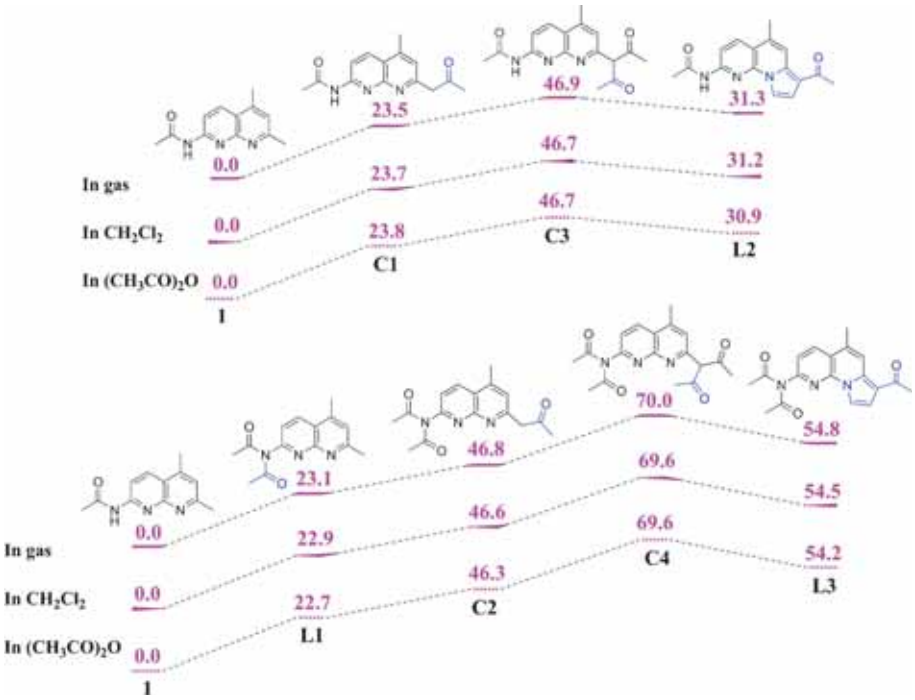

Figure 2. The calculated relative energies (kcal/mol) of **1**, **C1**-**C4**, **L1**-**L3** optimized under 6-311++G** level in different solvents.

Figure 3. DFT optimized structures and atomic charges of **1** at 6-311++G** level in different solvents.

and 445 nm (80%; 59 nm), respectively (Table 1). Although the emission bands of **L2**–**L4** occur at almost the same position, the quantum yields are similar. It may be due to their analogous extended structures and similar photoluminescence mechanism. Upon excitation at 388 nm, the solid emission spectra of **L2**–**L4** feature a broad and structureless peak with λ_{max} at 516 nm, 513 nm and 521 nm, respectively (Table 1). In order to research the fluorescence properties of pyrrolo[1′,5′-a]-1,8-naphthyridine (**L2**–**L4**) better, the Commission Internationale de L'Eclairage (CIE) coordinates were measured in CH_2Cl_2 and solid. The CIE coordinates measured in CH_2Cl_2 are (0.15, 0.10) for **L2**, (0.15, 0.08) for **L3** and (0.15, 0.06) for **L4**, respectively, which are nearly consistent with the international standard blue coordinates (0.15, 0.01); see in Figure 5 (left). And the CIE coordinates measured in solid are (0.22, 0.44) for **L2**, (0.25, 0.53) for **L3** and (0.25, 0.56) for **L4,** which are nearly consistent with the international standard kelly coordinates (0.22, 0.75); see in Figure 5 (right).

3.4 *Density Functional Theory Calculations*

To gain a deeper insight into the observed spectroscopic properties of **L1**–**L4**, density functional theory calculations were performed on these compounds with the Gaussian 09W package.[22] All geometrical structures were optimized with the 6-311++G** basis set. The UV-Vis spectra were computed from TD-DFT calculations in different media (gas, dichloromethane, acetic

Table 1. Optical properties of **L1**, **L2, L3** and **L4** in various solvents at 298 K.

Cpd.	Solvent	λ_{abs}/nm (ε/mol^{-1}dm^{3}cm^{-1})	λ_{em}/nm	Stokes shift/nm	[a]λ_{em}/nm	Φ_f
L1	*n*-hexane	318(8000)	n.d.	n.d.	n.d.	n.d.
	CH_2Cl_2	318(7875)				
	$CHCl_3$	317(8687)				
	CH_3CN	317(8583)				
	MeOH	318(9375)				
L2	*n*-hexane	291,388,410(23625)	425,447	59	516	0.76
	CH_2Cl_2	290,388,408(25083)	454	66		0.87
	$CHCl_3$	291,390,409(25373)	435,454	65		0.84
	CH_3CN	287,384,404(26125)	449	67		0.81
	MeOH	287,386,406(26650)	449	64		0.90
L3	*n*-hexane	292,389(21750)	427,448	59	513	0.68
	CH_2Cl_2	290,388(23125)	454	66		0.83
	$CHCl_3$	289,389(22578)	454	64		0.77
	CH_3CN	287,384(24562)	451	65		0.72
	MeOH	386,406(27100)	450	63		0.75
L4	*n*-hexane	288,367,385,406(24125)	419,440	55	521	0.76
	CH_2Cl_2	286,386,406(25416)	424,445	59		0.80
	$CHCl_3$	287,388,408(25775)	425,447	59		0.81
	CH_3CN	284,383,403(26250)	420,442	59		0.78
	MeOH	285,388,408(27300)	432	44		0.85

[a]solid state. n.d. = not detectable (signal too weak). φ = fluorescence quantum yield, calculated using quinine sulfate as standard ($\varphi = 0.546$ in 0.5 mol/L H_2SO_4).

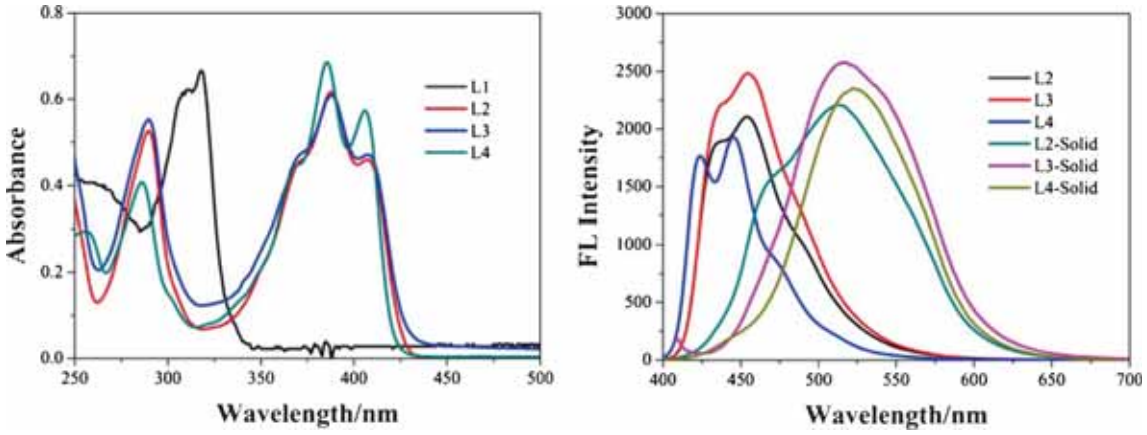

Figure 4. UV-Vis absorption and emission spectra of **L1**, **L2, L3** and **L4** in CH_2Cl_2 measured at a concentration of $\sim 1.0\times10^{-5}$ mol·L^{-1} and as solid.

anhydride) and the molecular orbitals were calculated in gas phase.

As shown in Figure 6 and Table 2, the calculated values of the absorption maximum (284.3 nm for **L1**, 394.5 nm for **L2**, 395.6 nm for **L3** and 384.2 nm for **L4** in CH_2Cl_2) agreed well with the experimental results in CH_2Cl_2. The deviation of absorption maximum between experimental and computational values are about 32 nm (10.3%), 6 nm (1.6%), 7 nm (1.9%) and 1.8 nm (0.4%), respectively. Figure 7 shows the electron distribution of the LUMO and HOMO for **L1–L4** and the related data are shown in Table 2. Clearly, the LUMO densities of **L1** are mainly located on the naphthyridine moiety and the HOMO densities too on the naphthyridine fragment. The LUMO densities of **L2–L4** are mainly located on the pyrrolo[1′,5′-a]-1,8-naphthyridine moiety and the HOMO densities too on the pyrrolo[1′,5′-a]-1,8-naphthyridine fragment (see Figure 7). This is further suggestive of local excitation (LE) of naphthyridine ring in **L1** and pyrrolo[1′,5′-a]-1,8-naphthyridine ring in **L2–L4**. The absorption intensity of **L1–L4** is contributed by the $S_0 \rightarrow S_1$, namely,

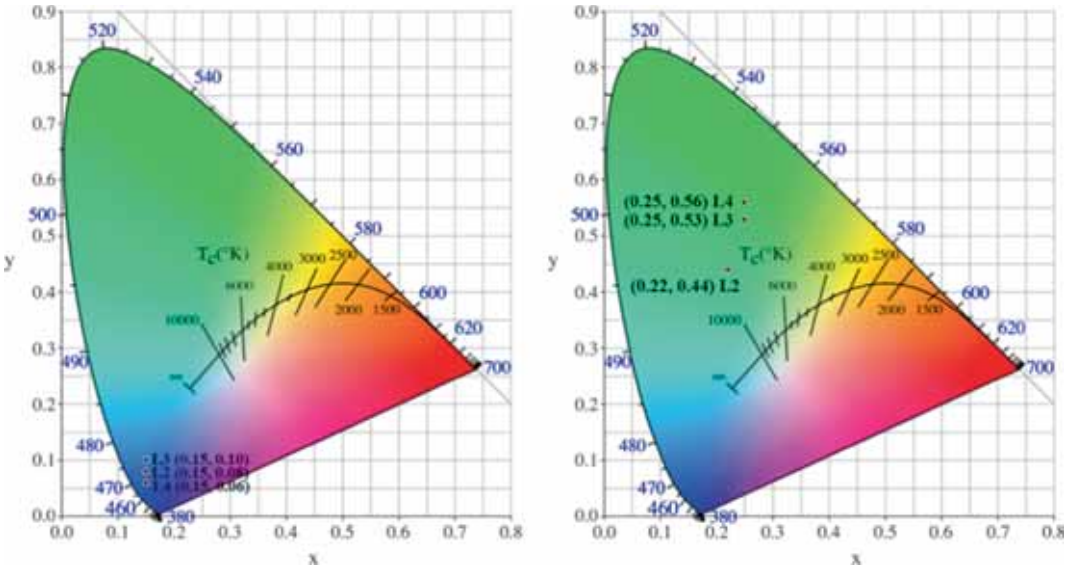

Figure 5. CIE-1931 chromaticity diagram of **L2**, **L3** and **L4** in CH_2Cl_2 (left) and in solid state (right).

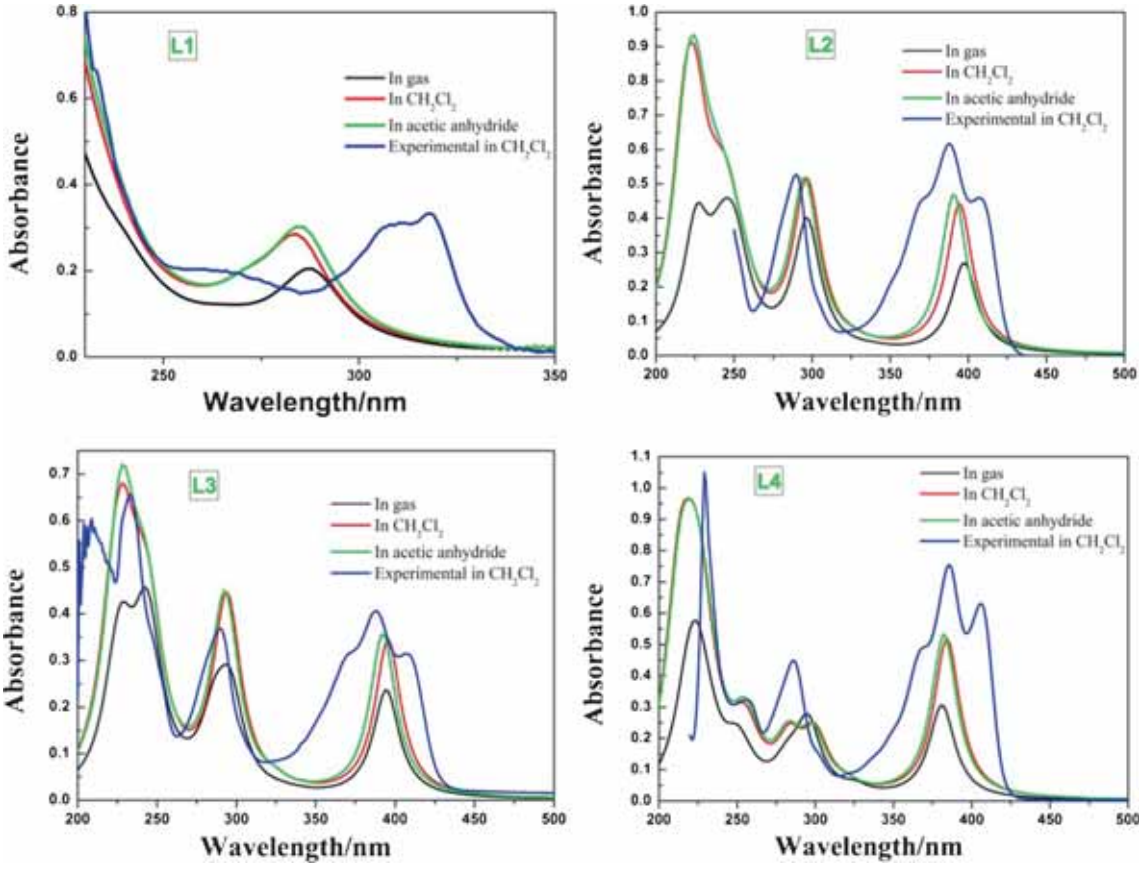

Figure 6. TD-DFT calculated UV-Vis spectra of **L1**, **L2, L3** and **L4** at B3LYP/6-311++G** level in different solvents and experimental spectra in dichloromethane.

HOMO to LUMO ($\pi \rightarrow \pi^*$) transition. The LUMO energy levels of **L1–L4** (−2.209, −2.035, −2.386 and −1.753 eV, respectively) are almost close, and the HOMO levels of **L2–L4** (−5.564, −5.961 and −5.381 eV) are close too. But the HOMO level of **L1** (−7.126 eV) is low compared to **L2–L4**.

Table 2. Absorption maxima, main orbital transitions, oscillator strengths (f) of **L1**, **L2, L3** and **L4** calculated by the TD-DFT B3LYP/6-311++G** level in different media.

Cpd.	Solution	Electronic transitions	Energy (eV)	[a]λ_{abs}/nm and λ_{abs}/nm	Error ratio (%)	Main orbital transition	f
L1	In gas	$S_0 \rightarrow S_1$	4.309	287.7	317(10.3%)	HOMO to LUMO (72.8%)	0.168
	In CH_2Cl_2	$S_0 \rightarrow S_1$	4.361	284.3			0.222
	In Ac_2O	$S_0 \rightarrow S_1$	4.342	285.5		HOMO to LUMO (76.6%)	0.239
						HOMO to LUMO (78.6%)	
L3	In gas	$S_0 \rightarrow S_1$	3.120	397.3	388(1.6%)	HOMO to LUMO (96.5%)	0.264
							0.433
	In CH_2Cl_2	$S_0 \rightarrow S_1$	3.143	394.5		HOMO to LUMO (97.9%)	0.460
	In Ac_2O	$S_0 \rightarrow S_1$	3.173	390.8			
						HOMO to LUMO (98.1%)	
L2	In gas	$S_0 \rightarrow S_1$	3.143	394.5	388(1.9%)	HOMO to LUMO (96.1%)	0.231
	In CH_2Cl_2	$S_0 \rightarrow S_1$	3.134	395.6			0.336
						HOMO to LUMO (97.5%)	
	In Ac_2O	$S_0 \rightarrow S_1$	3.159	392.4			0.349
						HOMO to LUMO (97.6%)	
L4	In gas	$S_0 \rightarrow S_1$	3.254	381.1	386(0.4%)	HOMO to LUMO (95.9%)	0.299
	In CH_2Cl_2	$S_0 \rightarrow S_1$	3.227	384.2			0.510
	In Ac_2O	$S_0 \rightarrow S_1$	3.242	382.5		HOMO to LUMO (97.9%)	0.524
						HOMO to LUMO (97.9%)	

[a]Experimental values measured in dichloromethane.

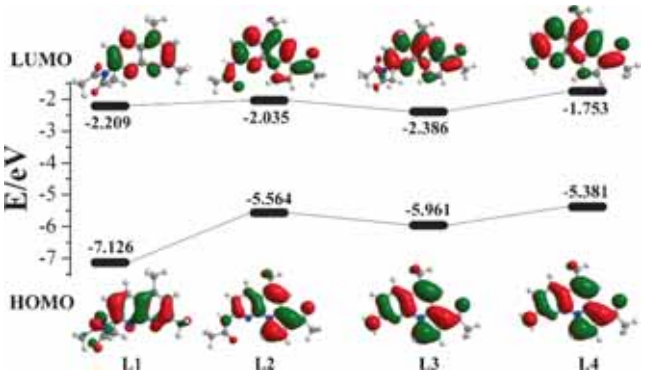

Figure 7. Molecular orbital energy diagrams and isodensity surface plots of the HOMO and LUMO of **L1**, **L2, L3, L4** calculated at B3LYP/6-311++G** level in gas.

4. Conclusions

In conclusion, we describe herein the syntheses, structures and spectroscopic properties of novel pyrrolo[1′,5′-a]-1,8-naphthyridine compounds (**L1–L4**) through a facile one-pot process. The possible synthetic mechanism of the reaction for **L2, L3** were studied by density functional theory calculations. The results showed that compounds **L2** and **L3** could be produced by the reaction of the corresponding 1,8-naphthyridines with aliphatic anhydride. Further, X-ray crystal analysis of 7-diacetamino-2,4-dimethy-1,8-naphthyridine (**L1**) identifies its molecular structure and reveals strong π–π stacking. The comprehensive studies of the spectroscopic properties are presented in various solvents and in solid state. Compound **L1** exhibited electronic absorption spectrum with λ_{max} at ~320 nm. **L2–L4** exhibited similar electronic absorption spectra with λ_{max} at ~390 nm that can be tentatively assigned to $\pi \rightarrow \pi^*$ transition arising from HOMO to LUMO, which is further supported by the results of density functional theory (DFT) calculations. Importantly, the understanding of the spectroscopic properties of **L1–L4** will be helpful to design novel pyrrolo[1′,5′-a]-1,8-naphthyridine compounds for biological and optical applications in future.

Supplementary information (SI)

Supplementary information associated with this article, *i.e.*, experimental procedures, characterization data, computational details, additional spectral data, and crystallographic data (CIF) are available at www.ias.ac.in/chemsci.

Acknowledgements

This work is supported by the National Natural Science Foundation of China (61361002, 21262049 and 21461007), the "Chun Hui" Plan of Chinese Ministry Education (Z2011125), the Scientific Research Foundation of Education Department of Yunnan Province (2013FZ121), the General Program of Yunnan Provincial Education Departmen (2015Y455), the Chemistry

of Key Construction Disciplines for Master Degree Program in Yunnan (HXZ1303) and the Educational Reform Program of Honghe University (JJJG1412).

References

1. Zou Y Q, Lu L Q, Fu L, Chang N J, Rong J, Chen J R and Xiao W J 2011 *Angew. Chem. Int. Ed.* **50** 7171
2. Feng C, Yan Y, Zhang Z, Xu K and Wang Z 2014 *Org. Biomol. Chem.* **12** 4837
3. Xiang L, Yang Y, Zhou X, Liu X, Li X, Kang X and Huang G 2014 *J. Org. Chem.* **79** 10641
4. Reissert A 1893 *Ber. Dtsch. Chem. Ges.* **26** 2137
5. Bera J K, Sadhukhan N and Majumdar M 2009 *Eur. J. Inorg. Chem.* 4023
6. Mahalingam M, Mohan P S, Gayathri K, Gomathi R and Subhapriya P 2013 *J. Chem. Sci.* **125** 1015
7. Kota T P and Kollipara M R 2014 *J. Chem. Sci.* **126** 1143
8. Wang C X, Sato Y, Kudo M, Nishizawa S and Teramae N 2012 *Chem-Eur. J.* **18** 9481
9. Hu S Z and Chen C F 2010 *Chem. Commun.* **46** 4199
10. Gan Q, Ferrand Y, Chandramouli N, Kauffmann B, Aube C, Dubreuil D and Huc I 2012 *J. Am. Chem. Soc.* **134** 15656
11. Yamazaki H, Hakamata T, Komi M and Yagi M 2011 *J. Am. Chem. Soc.* **133** 8846
12. Tseng H W, Zong R, Muckerman J T and Thummel R 2008 *Inorg. Chem.* **47** 11763
13. Bhuniya D, Umrani D, Dave B, Salunke D, Kukreja G, Gundu J, Naykodi M, Shaikh N S, Shitole P and Kurhade S 2011 *Bioorg. Med. Chem. Lett.* **21** 3596
14. Du M L, Hu C Y, Wang L F, Li C, Han Y Y, Gan X and Fu W F 2014 *J. Chem. Soc., Dalton Trans.* **43** 13924
15. Fernández-Mato A, Quintela J M and Peinador C 2012 *New J. Chem.* **36** 1634
16. Wu Y Y, Chen Y, Gou G Z, Mu W H, Lv X J, Du M L and Fu W F 2012 *Org. Lett.* **14** 5226
17. Boekelheide V and Windgassen R J 1959 *J. Am. Chem. Soc.* **81** 1456
18. Jones G and Stanyer J 1969 *J. Chem. Soc. C* **6** 901
19. Zhao X J, Chen Y, Fu W F and Zhang J B 2007 *Synth. Commun.* **37** 2145
20. Crosby G A and Demas J N 1971 *J. Phys. Chem.* **75** 991
21. Sheldrich G M 1997 *SHELX-97*, Program for the refinement of crystal structures, University of Gottingen, Germany
22. Frisch M J, Trucks G W, Schlegel H B, Scuseria G E, Robb M A, Cheeseman J R, Scalmani G, Barone V, Mennucci B, Petersson G A, Nakatsuji H, Caricato M, Li X, Hratchian H P, Izmaylov A F, Bloino J, Zheng G, Sonnenberg J L, Hada M, Ehara M, Toyota K, Fukuda R, Hasegawa J, Ishida M, Nakajima T, Honda Y, Kitao O, Nakai H, Vreven T, Montgomery J A, Peralta J E, Ogliaro F, Bearpark M, Heyd J J, Brothers E, Kudin K N, Staroverov V N, Keith T, Kobayashi R, Normand J, Raghavachari K, Rendell A, Burant J C, Iyengar S S, Tomasi J, Cossi M, Rega N, Millam J M, Klene M, Knox J E, Cross J B, Bakken V, Adamo C, Jaramillo J, Gomperts R, Stratmann R E, Yazyev O, Austin A J, Cammi R, Pomelli C, Ochterski J W, Martin R L, Morokuma K, Zakrzewski V G, Voth G A, Salvador P, Dannenberg J J, Dapprich S, Daniels A D, Farkas O, Foresman J B, Ortiz J V, Cioslowski J and Fox D J 2010 *Gaussian 09, Revision B.01*, (Gaussian, Inc.: Wallingford CT)
23. Raissi H, Yoosefian M, Moshfeghi E and Farzad F 2012 *J. Chem. Sci.* **124** 731
24. Tiwary A S and Mukherjee A K 2013 *J. Chem. Sci.* **125** 905
25. Becke A D 1988 *Phys. Rev. A* **38** 3098
26. Becke A D 1993 *J. Chem. Phys.* **98** 5648
27. Ghosh S, Girish K V S and Ghosh S 2013 *J. Chem. Sci.* **125** 933
28. Gou G Z, Zhou B, Shi L, Chi S M, Mang C Y and Liu W 2016 *Theor. Chem. Acc.* **135** 1
29. Hehre W J, Ditchfield R and Pople J A 1972 *J. Chem. Phys.* **56** 2257
30. Francl M M, Pietro W J, Hehre W J, Binkley J S, Gordon M S, DeFrees D J and Pople J A 1982 *J. Chem. Phys.* **77** 3654
31. Krishnan R, Binkley J S, Seeger R and Pople J A 1980 *J. Chem. Phys.* **72** 650
32. Gou G Z, Bo Z, Shi L, Xu S J, Yan H P, Liu W and Mang C Y 2015 *Indian J. Chem. A* **54** 1017
33. Miertuš S, Scrocco E and Tomasi J 1981 *Chem. Phys.* **55** 117
34. Gou G Z, Zhou B, Shi L, Chi S M, Chen X L and Liu W 2015 *Chin. J. Chem. Phys.* **28** 695
35. Henry R and Hammond P 1977 *J. Heterocyclic Chem.* **14** 1109
36. Brown E V 1965 *J. Org. Chem.* **30** 1607
37. Abranyi-Balogh P, Mucsi Z, Csizmadia I G, Dancso A, Keglevich G and Milen M 2014 *Tetrahedron* **70** 9682